جـامـعـة الـدوحـة
للعـلـوم والـتـكـنـولـوجـيـا
UNIVERSITY OF DOHA
FOR SCIENCE & TECHNOLOGY

AEMA 4311 Machine Design
Fall 2024

PROJECT REPORT

Topic: Stress Analysis, Design and Materials Selection for an Automotive Driveshaft to prevent failure and enhancing Performance

Student Name	Student ID
Abdul Wadood Fathah	60104538
Mohammed Abdelkarim	60104560
Mohammed Abdelshafie	60087589
Majad Al-Sharshani	60072016
Ragab Efhied	60101239

Instructor: Rizwan Saeed Choudhry
Date of Submission: November 28, 2024

Executive Summary

This project focuses on the design and material selection for an automotive driveshaft, aimed at reducing weight and improving performance for motorsport applications while minimizing environmental impact. The failure analysis of the half-shaft from the Formula SAE racing car, as outlined in the study by Guimaraes et al., served as a valuable reference for our project. The study highlighted the importance of material selection, stress concentration, and fatigue analysis, particularly at critical areas like the spline roots. The reference shaft, made from Low Alloy Steel AISI 4140, was used as a baseline for comparison, with the goal of reducing its mass by at least 40%. A thorough material selection process was conducted using Ansys Granta EduPack, where the material, Low Alloy Steel AISI 9255, was chosen based on its superior yield strength, fracture toughness, and lower density, which directly contributed to a 44.6% reduction in the shaft's mass. The design incorporated a hollow structure to achieve weight reduction without compromising strength. Detailed stress and buckling analyses were performed using Finite Element Analysis (FEA) to simulate real-world conditions and assess the shaft's ability to withstand the applied loads. The stress analysis focused on identifying critical stress concentrations, particularly at the spline root, and confirmed that the maximum stress was well below the material's yield strength, ensuring the shaft would not fail under operational torque. The buckling analysis evaluated the shaft's stability under different support conditions, with the pin-pin configuration providing a conservative estimate of the shaft's load-bearing capacity. The results demonstrated that the shaft could endure significantly higher loads than those expected in typical use. The environmental impact of both materials was assessed, showing that AISI 9255 reduces energy use by 27% and CO2 footprint by 25% compared to AISI 4140. This is mainly due to a more efficient production process and lighter weight, which lowers energy consumption during operation. Although manufacturing and transportation stages have slightly higher energy use, the overall environmental benefits of AISI 9255 align with the goal of creating a sustainable, high-performance driveshaft. This design ensures that the new shaft meets performance criteria, including torque transmission, deflection limits, and cost constraints, while making significant strides toward sustainability and efficiency in motorsport engineering.

Table of Content

List of Figures

List of Tables

1. Embodiment level design

Material Selection Problem Formulation

Function:
To design a lightweight, cost-effective, and durable replacement motorsport car drive shaft that can withstand specified torque and angle of twist while ensuring compatibility with existing couplings and transmission.

Objectives:

1. Minimize mass: The mass of the new shaft must be reduced by at least 40% compared to the reference shaft (i.e., reduced to 1.68 kg or less).
2. Minimize cost: The material and processing cost should not exceed £500 per shaft.

Constraints:

- Shaft Length L = 0.5m is fixed
- Ability to transmit a maximum torque T = 950 Nm without yielding, i.e. $\tau < \sigma_y$
- Maximum angle of twist $\phi \leq 10°$
- Shaft Outer radius r = 15 mm is fixed

Material indices:
To maximize performance while minimizing mass, we use the following indices:

1. For strength $M_1 = (\frac{\sigma_y}{\rho})$

   Where: σ_y = Yield strength of the material.
   ρ = Density of the material.

2. For stiffness $M_2 = (\frac{G}{\rho})$

   Where: G = Shear modulus of the material.

Results of Material Selection Study at Embodiment Level

Stage 1: Chart - Yield Strength / Density vs. Shear Modulus / Density
The Figure 1 chart presents the material selection results for the optimal design of the replacement drive shaft. The materials suitable for the shaft fall in regions where both indices (σy/ρ and G/ρ) are maximized, aligning with the objective of lightweight, strong, and stiff materials. The **X-axis** represents the Shear Modulus-to-Density ratio, which measures stiffness relative to weight—critical for minimizing deflection and ensuring structural integrity. The **Y-axis** represents the Yield Strength-to-Density ratio, which measures strength relative to weight—essential for resisting failure under applied torque. This chart highlights materials in the top left quadrant, where the material indices are maximized. This region is primarily occupied by composites, fibers and particulates, and certain high-performance alloys, which exhibit excellent strength and stiffness relative to their density. These materials are well-suited for achieving significant weight reduction while maintaining performance. After this embodiment design, which identifies the optimal material candidates, we will proceed with detailed design to finalize the material selection.

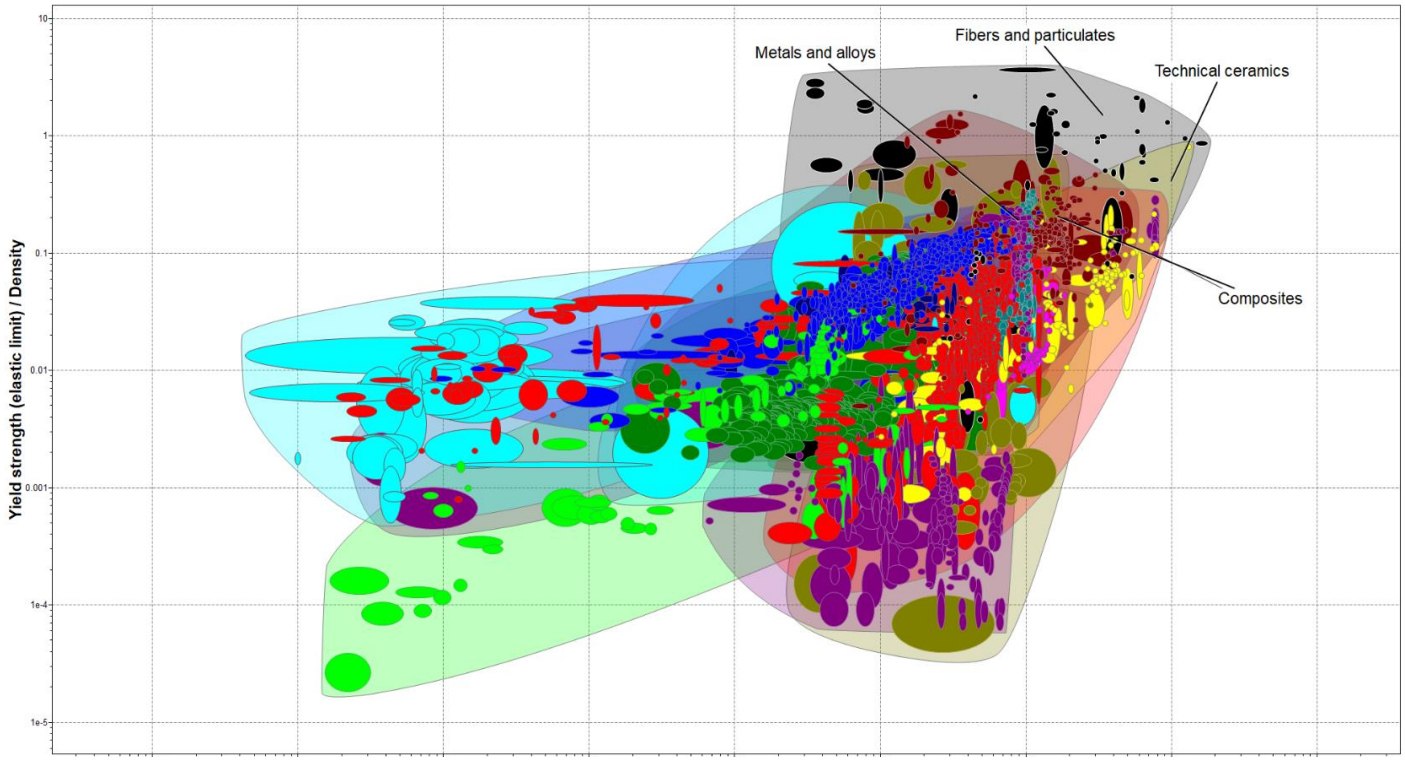

Figure 1 Stage 1 Chart

2. Detailed Design

Mathematical Calculations:

T = 950 Nm
ϕ = 10° * (π/180) = 0.1745 radians
D = 0.03 m, r_o = D/2 = 0.03m/2 = 0.015 m
L = 0.5 m

Assuming an inner diameter of 0.02 m for a reasonable estimation for stress distribution.

$$J = \frac{\pi(D^4 - d^4)}{32} = \frac{\pi(0.03^4 - 0.02^4)}{32} = 6.38136 \times 10^{-8} m^4$$

Calculating Constraint on strength:

$$Shear\ stress\ due\ to\ torsion\ \tau = \frac{Tr_o}{J} = \frac{950\ Nm * 0.015m}{6.38136 \times 10^{-8} m^4} = 223.3066\ MPa$$

$$Maximum\ stress\ concentration\ factor\ due\ to\ spline\ for\ a\ round\ shaft\ is\ K_t = 5$$
$$\tau_{max} = \tau * K_t = 223.3066\ MPa * 5 = 1.1165\ GPa$$

$$Minimum\ yield\ strength\ \sigma_y = 2\tau_{max} = 2 * 1.1165\ GPa$$
$$= \mathbf{2.233\ GPa}\ [Tresca\ Criteria]$$

Calculating Constraint on Deflection:

$$Angle\ of\ twist\ due\ to\ torsion\ \phi = \frac{TL}{JG}$$

$$Rearranging\ to\ find\ minimum\ Shear\ Modulus$$
$$\Rightarrow G = \frac{TL}{J\phi} = \frac{950\ Nm * 0.5\ m}{6.38136 \times 10^{-8} m^4 * 0.1745} = \mathbf{42.65\ GPa}$$

Identifying Maximum density:

$$A = \frac{\pi(D^2 - d^2)}{4} = \frac{\pi(0.03^2 - 0.02^2)}{4} = 3.927 \times 10^{-4} m^2$$
$$V = AL = (3.927 \times 10^{-4}) m^2 \times 0.5m = 1.9635 \times 10^{-4} m^3$$

$$m_{max} = 2.8kg - \left(\frac{40}{100} * 2.8kg\right) = 1.68kg$$
$$\rho_{max} = \frac{m_{max}}{V} = \frac{1.68kg}{1.9635 \times 10^{-4} m^3} = 8556.1697 kg/m^3$$

Choosing the Inner Radius and Fillet Radius:

To reduce mass, while keeping the outer radius fixed at 0.015 m, we made the shaft hollow and selected an inner radius of 0.01m. This design choice effectively reduces the shaft's mass by removing excess material from the center, achieving the required weight reduction without compromising strength. The inner radius of 0.01 m ensures that the shaft maintains sufficient structural integrity to transmit the maximum torque without yielding, while also limiting the angle of twist.

For the selection of material, we chose the highest Kt = 5, which gives a fillet radius of 0.3mm ensuring that the material is capable of withstanding extreme stress concentrations. For the actual design we will choose the lowest Kt = 3, which gives a larger fillet radius of 1.2mm, which lowers stress risers and leads to more uniform stress distribution. This conservative approach provides an additional margin of safety ensuring the drive shaft can withstand worst-case scenarios, including manufacturing imperfections and extreme loads.

Results of Material Selection Study at Detailed Level:

Stage 2: Constraints - Yield Strength (Elastic Limit) and Shear Modulus
In this stage, we apply the constraints based on the calculated yield strength and shear modulus for the material.

- **Yield Strength ≥ 2.23e3 MPa** ensures the material can handle the maximum torque without permanent deformation.
- **Shear Modulus ≥ 42.6 GPa** ensures the material is stiff enough to avoid excessive twisting (minimizing the angle of twist).

Stage 3: Chart - Mass per unit of stiffness vs. Price (EUR/kg)
The Figure 3 chart compares the mass per unit of stiffness with the cost per kilogram, helping to identify materials that offer the best trade-off between performance (in terms of stiffness and weight) and cost. The goal is to find materials that are both high-performing and cost-effective. As part of Stage 2, the calculated constraints for yield strength and shear modulus were applied, resulting in only a few materials passing through. The chart shows that some metals and alloys, as well as composites, fibers, and particulates, meet these requirements.

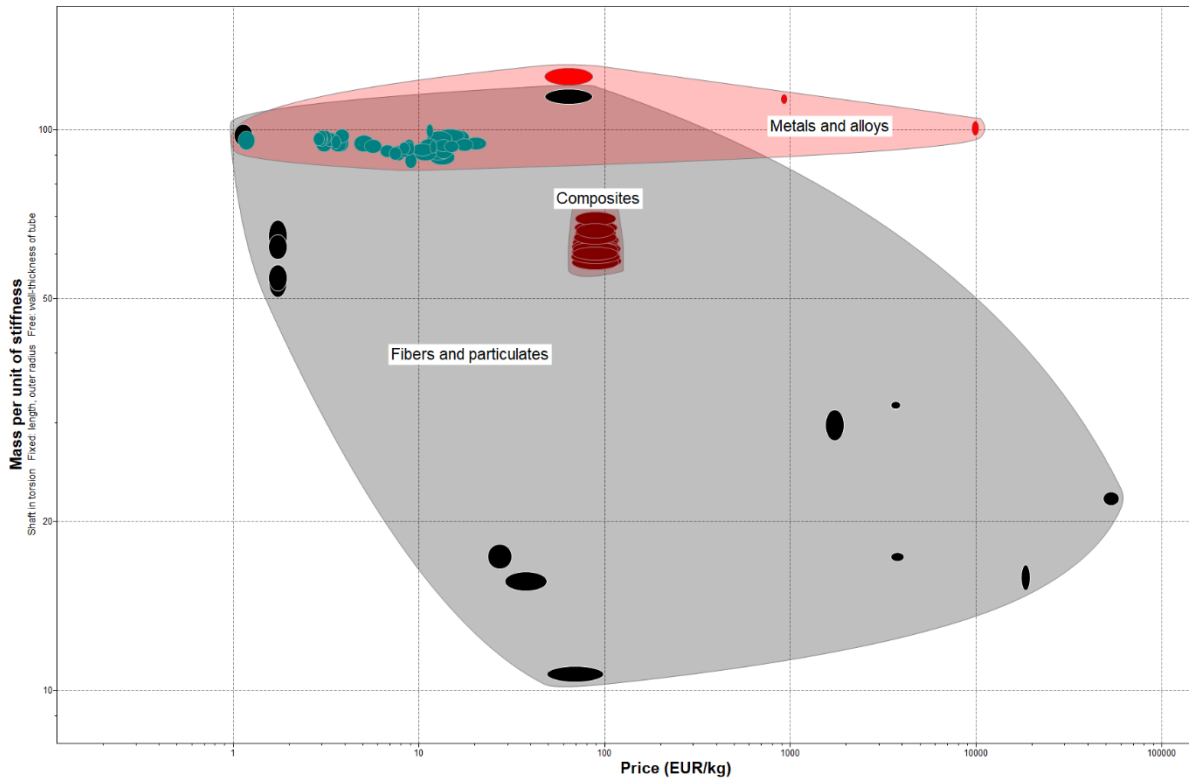

Figure 2 Stage 3 Chart

Stage 4: Tree - Process Universe - Shaping/Machining
This stage evaluates the **processability** of the remaining materials. The "Process Universe" tree categorizes materials based on their machinability and suitability for the desired manufacturing processes. After this stage, the materials are limited to those that can be effectively shaped and machined according to the project's needs. By this point, the remaining materials are mostly metal alloys.

Stage 5: Chart- Fracture Toughness / Density vs. Price (EUR/kg)

Stage 5 focuses on evaluating materials based on their fracture toughness-to-density ratio and price per kilogram. This stage ensures that selected materials can resist crack propagation while maintaining low weight, offering a balance between durability and cost-effectiveness

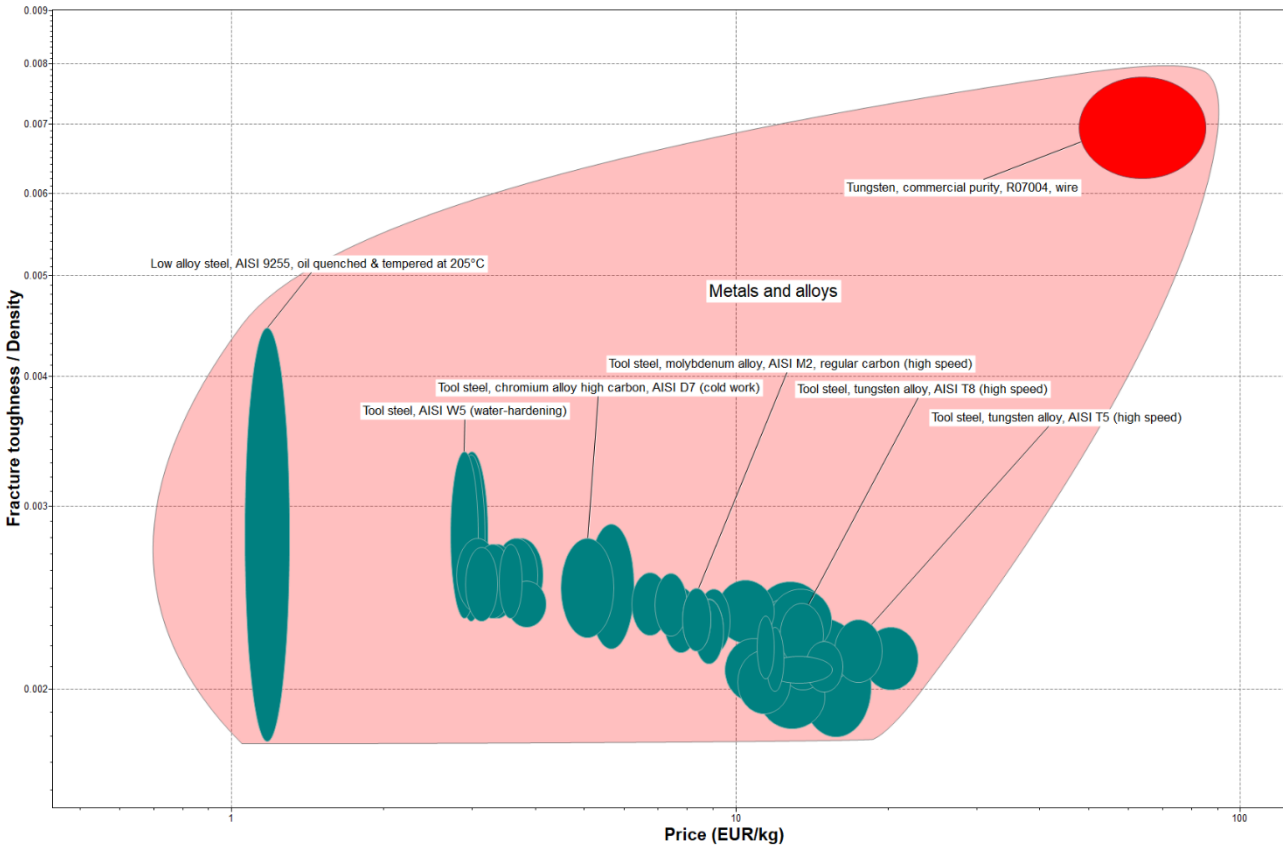

Figure 3 Stage 5 Chart

	Low alloy steel, AISI 9255, oil quenched & tempered at 205°C	Tool steel, molybdenum alloy, AISI M44 (high speed)	Tool steel, molybdenum alloy, AISI M43 (high speed)
Computed Properties			
Yield strength (elastic limit) / Density	0.234 - 0.287	0.249 - 0.327	0.28 - 0.333
Shear modulus / Density	0.0101 - 0.0108	0.00999 - 0.0106	0.01 - 0.0107
Mass per unit of stiffness	92.3 - 99.4	94.3 - 100	93.7 - 99.5
Fracture toughness / Density	0.00178 - 0.00446	0.0018 - 0.00225	0.00183 - 0.00211
Price			
Price (EUR/kg)	1.06 - 1.3	13.4 - 18.5	11.1 - 14.9
Physical properties			
Density (kg/m^3)	7800 - 7900	8510 - 8680	8360 - 8530
Mechanical properties			
Yield strength (elastic limit) (MPa)	1840 - 2260	2140 - 2810	2370 - 2810
Shear modulus (GPa)	79 - 85	86 - 91	85 - 90
Fatigue strength at 10^7 cycles (MPa)	668 - 771	641 - 843	711 - 843
Impact & fracture properties			
Fracture toughness (MPa.m^0.5)	14 - 35	15.5 - 19.3	15.5 - 17.8

Table 0-1 Comparison between top 3 Material

Table 1 compares the top three materials considered for the replacement drive shaft after Stage 5: Low Alloy Steel AISI 9255, Tool Steel AISI M44, and Tool Steel AISI M43. While Tool Steel AISI M44 and Tool Steel AISI M43 offer higher yield strength, shear modulus, fatigue strength, and fracture toughness, Low Alloy Steel AISI 9255 stands out due to its significantly lower cost and density. The lower density of AISI 9255 helps in achieving a lighter shaft, directly contributing to meeting the objective of reducing the mass by at least 40%. Its cost-effectiveness ensures that the material and processing cost remains within the specified budget of £500 per shaft. Therefore, despite the superior mechanical properties of the tool steels, Low Alloy Steel AISI 9255 is good choice for meeting both mass and cost objectives.

Stage 6: Tree - Shape Universe - Plain hollow axisymmetric prism

Stage 6, the "Shape Universe," focuses on selecting materials that can be formed into the required "plain hollow axisymmetric prism" shape for the drive shaft. This stage ensures that the material can be effectively processed into a hollow cylindrical shape with the necessary dimensions, considering manufacturability and material properties like ductility and machinability. After applying these shaping constraints, Tool Steels AISI M44 and AISI M43 did not pass through Stage 6 due to limitations in their machinability and ductility, making them unsuitable for forming the desired geometry. As a result, only Low Alloy Steel AISI 9255 remained as the optimal material, meeting all the performance, cost, and manufacturing criteria for the drive shaft.

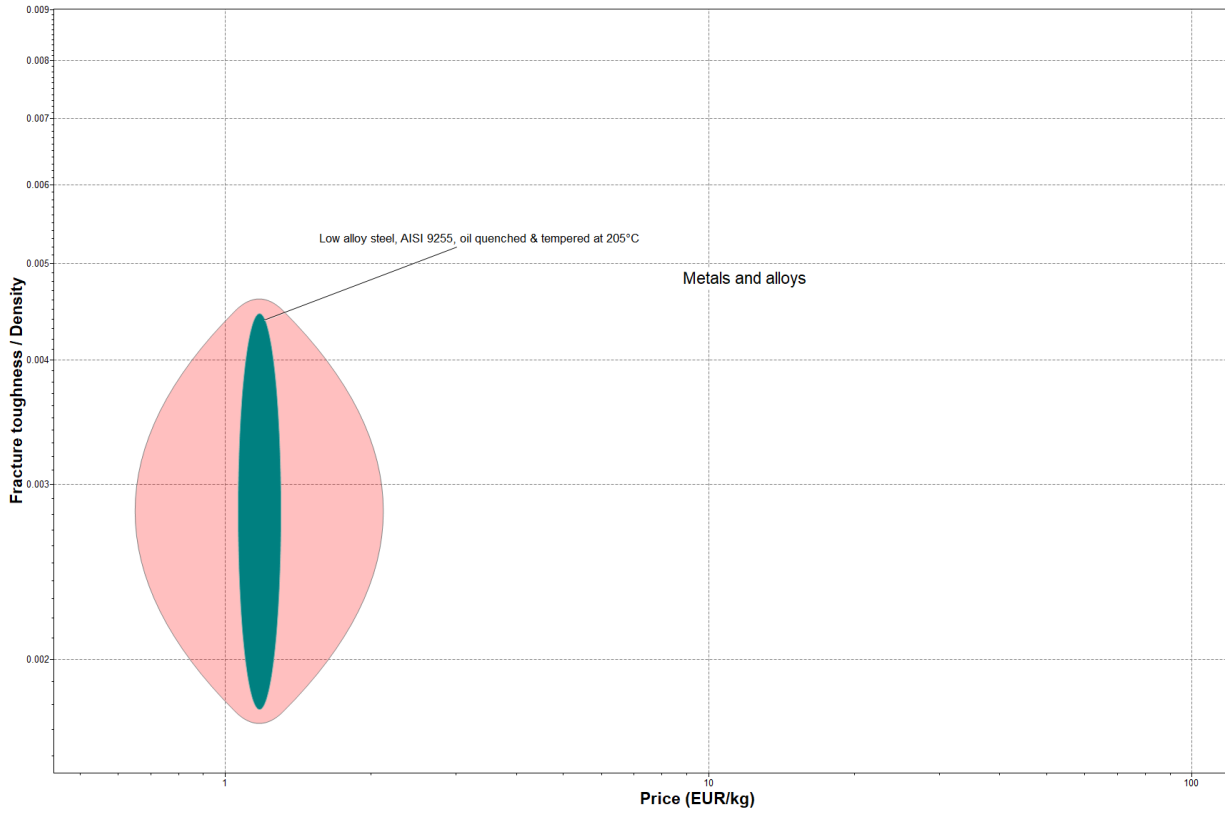

Figure 4 Chart based on Stage 6

Final Selection:

	Low alloy steel, AISI 9255, oil quenched & tempered at 205°C	Low alloy steel, AISI 4140, oil quenched & tempered at 650°C
Computed Properties		
Yield strength (elastic limit) / Density	0.234 - 0.287	0.0758 - 0.0911
Shear modulus / Density	0.0101 - 0.0108	0.0102 - 0.0108
Mass per unit of stiffness	92.3 - 99.4	92.3 - 98.2
Fracture toughness / Density	0.00178 - 0.00446	0.00637 - 0.0102
Price		
Price (EUR/kg)	1.06 - 1.3	1.07 - 1.33
Physical properties		
Density (kg/m^3)	7800 - 7900	7800 - 7900
Mechanical properties		
Yield strength (elastic limit) (MPa)	1840 - 2260	595 - 715
Shear modulus (GPa)	79 - 85	80 - 85
Fatigue strength at 10^7 cycles (MPa)	668 - 771	326 - 379

Table 0-2 Comparison between Selected material (Low alloy steel, AISI 9255) and Reference material (Low alloy steel, AISI 4140)

Tabele 2 shows that the Selected material (Low alloy steel, AISI 9255) and Reference material (Low alloy steel, AISI 4140) has similar cost, density, and shear modulus. But AISI 9255 has much higher yield strength and fatigue strength.

$$m_{selected\ material} = V_{hollow\ shaft} \times \rho_{selected\ material}$$
$$= (1.9635 \times 10^{-4} m^3) \times 7900 kg/m^3 = 1.5512 kg$$

$$\%mass\ reduced\ = \frac{(2.8kg - 1.5512kg)}{2.8} \times 100 = 44.6\%$$

The result shows a mass reduction of 44.6% by selecting the chosen material, which significantly contributes to meeting the goal of reducing the drive shaft's mass by at least 40%.

FEA Stress Analysis

In the stress FEA analysis of the splined motorsport drive shaft with the selected material and an applied torque of 950 Nm, the maximum stress of 1.035×10^9 Pa occurs at the spline root, which is a common location for stress concentration due to the sharp transition between the shaft and the spline. This high stress at the spline root is expected, as it is a critical area where the geometry creates a localized concentration of forces. The minimum stress of 1.695×10^8 Pa is found at the top part of the spline, where the geometry is less prone to stress concentration. Since the maximum stress at the spline root is well below the material's yield strength of 2.037×10^9 Pa, this indicates that the drive shaft will not fail under the applied load. The design is safe, with the material capable of handling the torque without yielding, even at the highest stress concentration point.

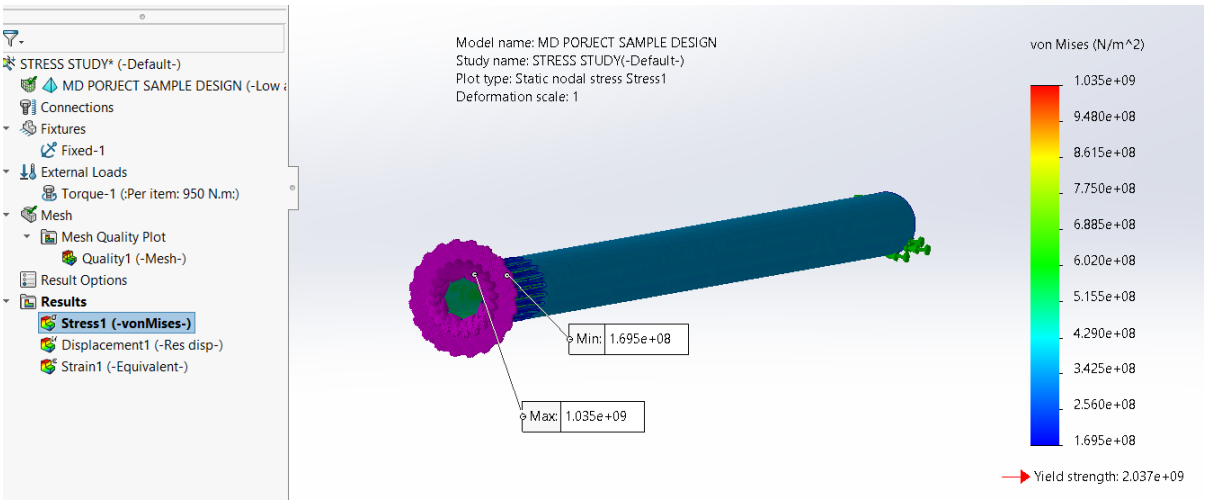

Figure 5 FEA Stress Analysis of splined shaft

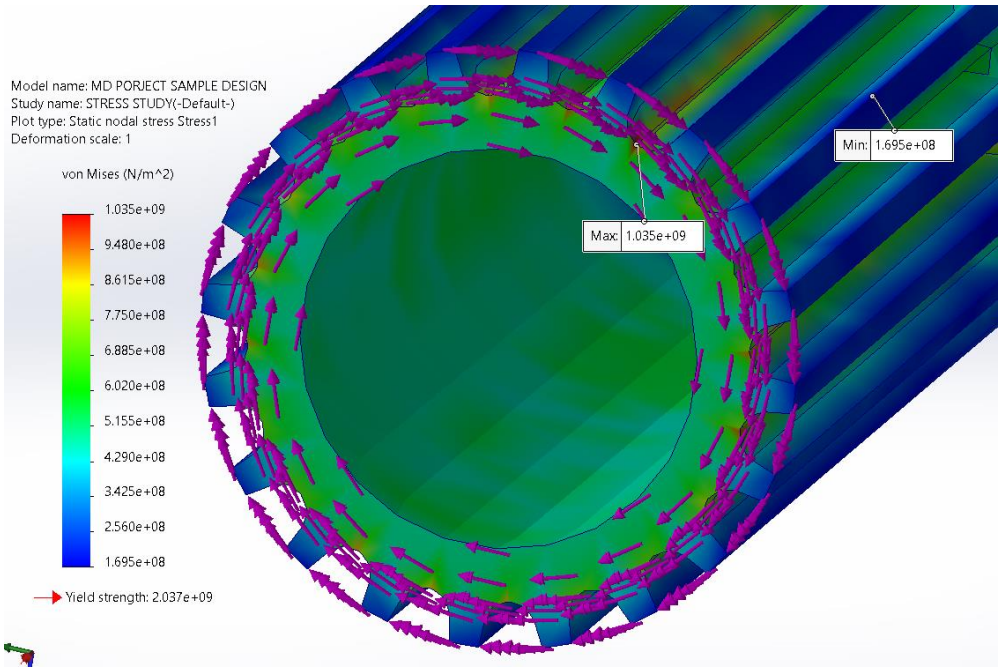

Figure 6 Close up of FEA Analysis

FEA Buckling Analysis

We performed two buckling analyses, one with a pin-pin condition and another with a free-pin condition, to assess the drive shaft's stability under different support configurations. The pin-pin condition represents a more rigid setup with supports at both ends, providing a more accurate and conservative estimate of the shaft's buckling resistance in real-world applications. The free-pin condition, on the other hand, simulates a more flexible scenario with one free end, helping to evaluate the shaft's behavior under less constrained conditions. We did not include splines in the model to reduce simulation time; however, this simplification does not significantly affect the overall results, as the focus was on the general buckling behavior of the shaft.

In the pin-pin condition, the drive shaft is assumed to be supported at both ends, which mimics a more rigid setup, such as a shaft fixed in bearings. The split line technique was used to simulate the pin-pin condition, effectively applying the appropriate boundary conditions to represent the shaft's support at both ends. This approach helps to accurately predict the shaft's behavior under load, providing reliable results for the buckling analysis. The analysis shows a load factor of 9596, indicating that the shaft can withstand approximately 9596 times the applied torque before buckling would occur. This suggests a very high tolerance for applied loads, indicating that the shaft is well-supported and has a strong resistance to buckling. The amplitude of 8.447×10^{-3} represents the maximum deflection or deformation of the shaft, which is relatively small, further confirming that the shaft remains stable under the applied load.

In the free-pin condition, one end of the drive shaft is fixed while the other is free to move. This is a more flexible support configuration which allows for greater potential deformation. The results show a much lower load factor of 0.09596, meaning the shaft can withstand only about 1/10th of the torque before buckling becomes a concern. The free-pin condition result is helpful as it provides insight into the shaft's behavior under less constrained conditions, offering a broader understanding of its performance in scenarios where one end may be unsupported or more flexible.

Comparing both conditions, the pin-pin condition offers a more conservative and reliable estimate of the shaft's ability to withstand loads without buckling, making it a more accurate and safer representation of real-world applications where both ends are likely supported. The results of the buckling analysis show that under the applied torque of 1 Nm, the shaft can withstand much higher loads without buckling, which suggests that the chosen material and design will hold up to the 950 Nm torque applied in the real-world scenario without failing due to buckling. The material's high load factor in the pin-pin condition and the low deflection indicate that the shaft will maintain its structural integrity even under extreme conditions.

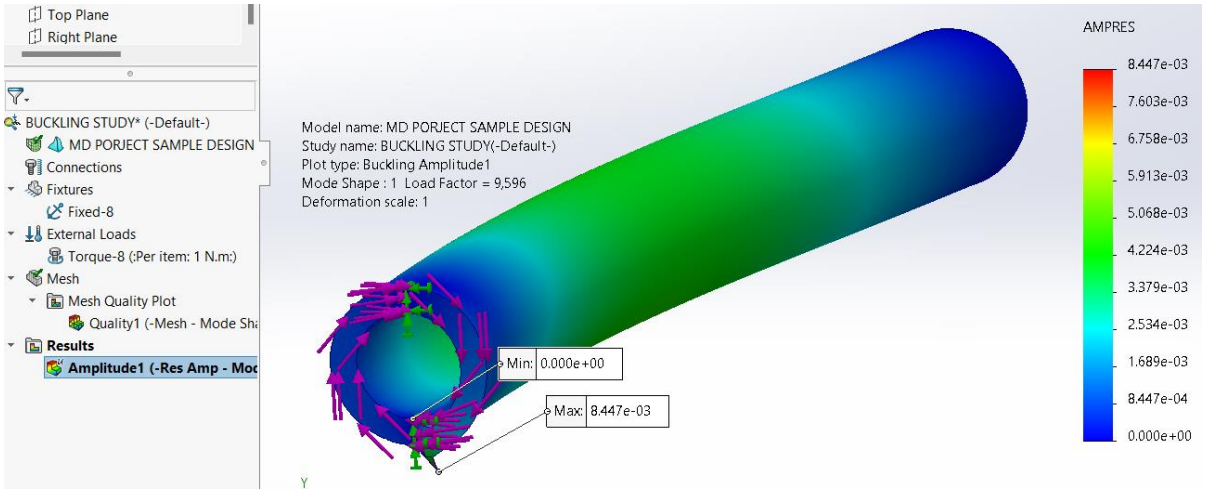

Figure 7 FEA Buckling Analysis Pin-Pin Condition

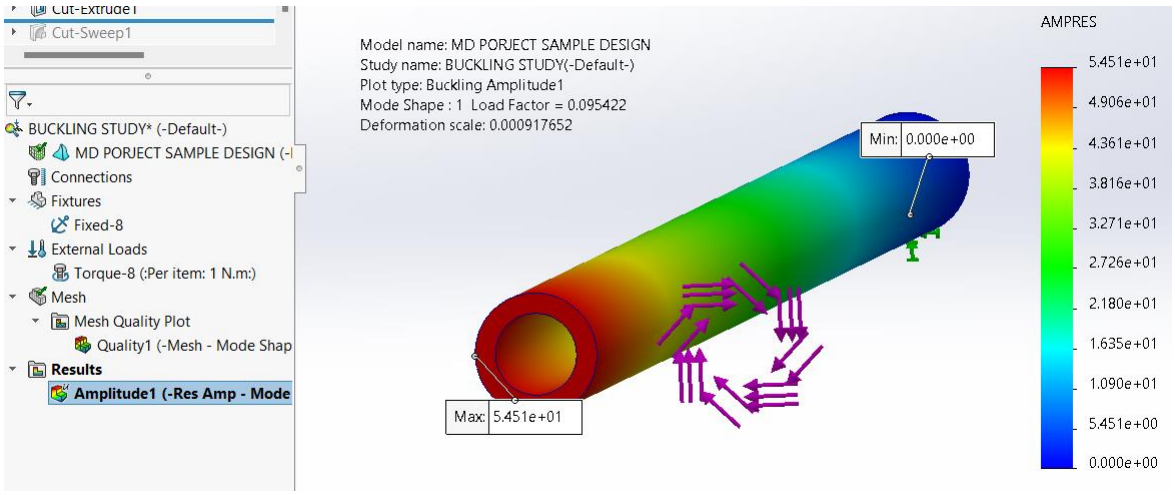

Figure 8 FEA Buckling Analysis Free-Pin Condition

The FEA stress and buckling analyses confirm that the selected material and design of the drive shaft can withstand the applied torque without yielding or buckling. The results show that the shaft remains stable under extreme loading conditions, ensuring its structural integrity and reliability for real-world applications.

Environmental Impact Comparison

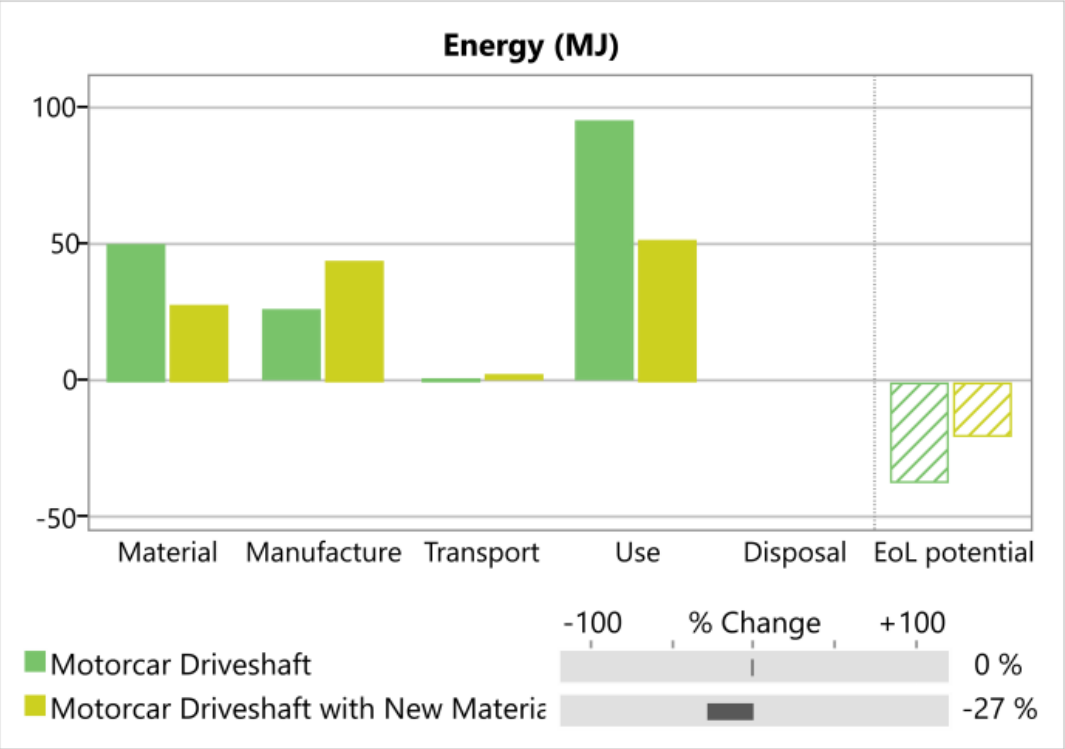

Figure 9 Comparison of Energy Use of the Reference material and New material

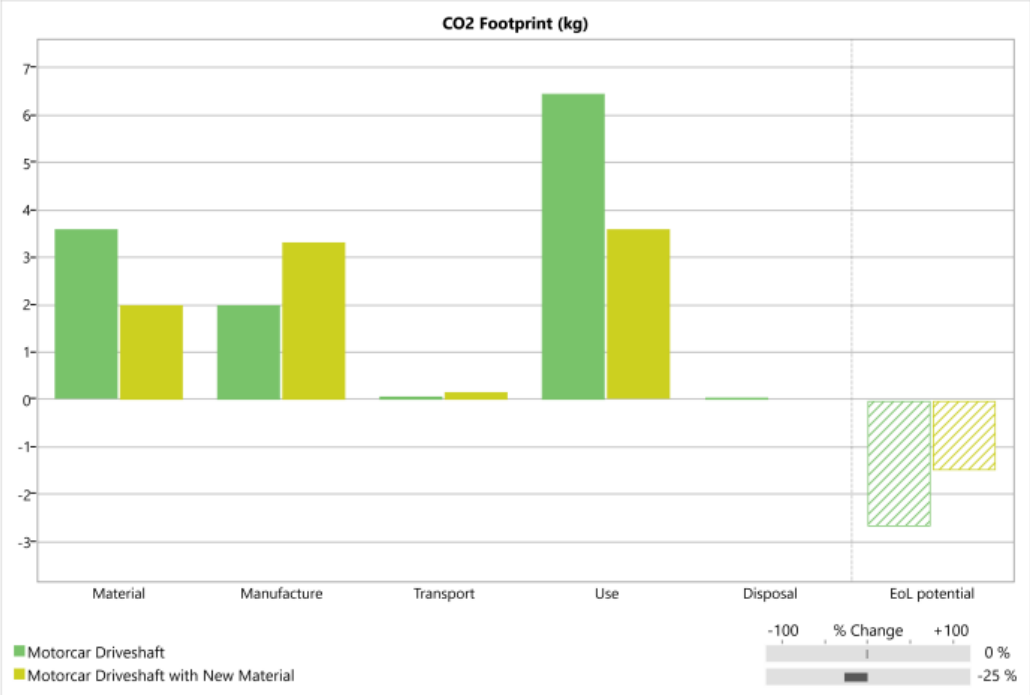

Figure 10 Comparison of CO2 emission of the Reference material and New material

Phase	Energy (MJ)	Energy (%)	CO2 footprint (kg)	CO2 footprint (%)
Material	50.6	29.1	3.58	29.4
Manufacture	26.6	15.3	1.99	16.4
Transport	1.01	0.6	0.0784	0.6
Use	95.2	54.7	6.47	53.2
Disposal	0.56	0.3	0.0392	0.3
Total (for first life)	**174**	**100**	**12.2**	**100**
End of life potential	-38		-2.69	

Table 0-3 Reference Material Environmental Impact

Phase	Energy (MJ)	Energy (%)	CO2 footprint (kg)	CO2 footprint (%)
Material	28	21.9	1.98	21.8
Manufacture	44.3	34.7	3.33	36.6
Transport	2.5	2.0	0.172	1.9
Use	52.7	41.2	3.58	39.5
Disposal	0.31	0.2	0.0217	0.2
Total (for first life)	**128**	**100**	**9.08**	**100**
End of life potential	-21		-1.49	

Table 0-4 New Material Environmental Impact

We analyzed the environmental impact of the reference material, Low Alloy Steel AISI 4140 (oil quenched & tempered at 650°C), and the selected material, Low Alloy Steel AISI 9255 (oil quenched & tempered at 205°C), using the ANSYS Granta EduPack ECO Audit tool. This analysis focused on energy use and CO2 footprint across several stages of the material lifecycle: production, manufacturing, transportation, use in the car, and end-of-life potential. We made reasonable assumptions for each stage of the material lifecycle to ensure a comprehensive evaluation of their environmental impact.

For material production, the selected material (AISI 9255) shows a lower energy use and CO2 footprint compared to the reference material (AISI 4140). This is likely due to the more efficient production process associated with AISI 9255, which requires less energy during extraction and processing, possibly because of its lower alloying content and tempering process at a lower temperature (205°C vs. 650°C), which consumes less energy.

During the manufacturing stage (forging and machining), the reference material (AISI 4140) has a lower energy use and CO2 footprint compared to the selected material (AISI 9255). This could be because AISI 4140 is a more commonly used material, leading to optimized and more energy-efficient manufacturing processes. In contrast, AISI 9255 might require more energy-intensive processes or specialized techniques, such as more complex forging or machining operations, which contribute to a higher footprint.

In terms of transportation, the selected material (AISI 9255) results in higher energy use (MJ) and a larger CO2 footprint (kg). This could be due to the fact that AISI 9255 might be less widely available, requiring longer or more complex transportation routes, or possibly heavier or bulkier shipments due to its different form or alloy composition.

For the use in the car, the selected material (AISI 9255) demonstrates lower energy use and CO2 footprint. This is likely due to its lighter weight and superior strength-to-weight ratio, which leads to a more efficient drive shaft, reducing overall energy consumption and CO2 emissions during the car's operation.

Finally, regarding end-of-life potential, the selected material (AISI 9255) has a lower environmental impact, which could be due to better recyclability or more sustainable disposal practices compared to the reference material. This means less energy is required to recycle or dispose of the selected material at the end of the vehicle's life.

Overall, the selected material (AISI 9255) results in a 27% reduction in total energy consumption and a 25% reduction in CO2 footprint compared to the reference material (AISI 4140). These improvements are mainly driven by the lower energy requirements during material production and use in the car, despite the higher energy use and CO2 footprint during manufacturing and transportation stages. This reduction in environmental impact aligns with the goal of designing a more sustainable, high-performance drive shaft for the motorsport car.

3. References

https://www.sciencedirect.com/science/article/pii/S2213290216300086

http://www.volkspage.net/technik/manuaisecatalogos/02/automotivetransmissions_fundamentalsselectiondesignandaplication.pdf

https://app.knovel.com/web/view/khtml/show.v/rcid:undefined/cid:kt012EDHKF/viewerType:khtml//root_slug:miscellane-charts/?view=collapsed

https://www.researchgate.net/publication/309329869_Design_and_Analysis_of_Drive_Shaft_of_an_Automobile

https://www.wiley.com/en-us/Fundamentals+of+Machine+Component+Design%2C+7th+Edition-p-9781119475682

Peterson’s Stress Concentration Factors Second Edition
https://d1n7iqsz6ob2ad.cloudfront.net/document/pdf/532c520a9d92c.pdf

https://www.ansys.com/content/dam/amp/2021/august/webpage-requests/education-resources-dam-upload-batch-6/performance-indices-booklet-bokpeien22.pdf

https://www.geartechnology.com/ext/resources/issues/0919x/spline-design.pdf